and the output $5f_T/4$. Because the magnification of such a system is negative (−4), we would expect a pulse to be reversed in time at the output. To test this hypothesis we imaged two pulses separated by 20 ps. The input pulse width was 1·5 ps for each of the two pulses, which was less than the 6 ps resolution of the time lens, but was required in order to accommodate the 30 ps aperture time. Input and output waveforms illustrating time reversal were measured with a New Focus Model 1014 detector connected to an HP 71500A microwave transition analyser and were system limited to 20 ps FWHM. Fig. 3 illustrates the two input pulses with the weaker pulse delayed 20 ps with respect to the strong pulse. Fig. 4 illustrates time reversal: the weaker pulse is now advanced with respect to the stronger pulse, as verified by blocking the weaker pulse at the input. Furthermore, a magnification of −4 was verified by noting that the separation between the two pulses changed from 20 to 80 ps.

In conclusion, we have demonstrated the time-reversal imaging and jitter suppression properties of a temporal imaging system. These two simple experiments exemplify the

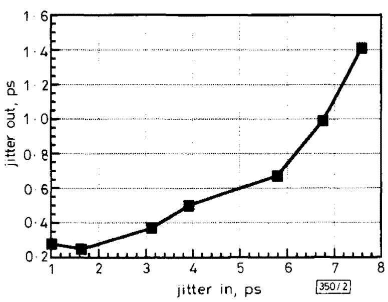

Fig. 2 *Measured RMS pulse jitter at output of time lens against RMS jitter measured at input*

A focusing geometry is used

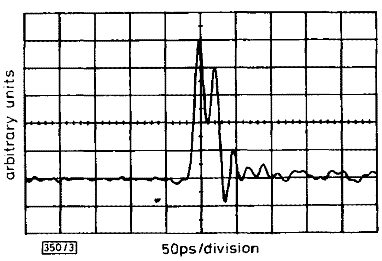

Fig. 3 *Measured pulse pair input to time-lens imaging system*

The weaker pulse is delayed 20 ps with respect to the stronger pulse

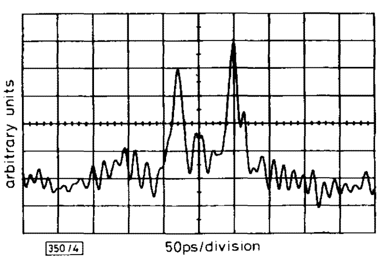

Fig. 4 *Measured pulse pair output from time-lens imaging system*

The weaker pulse now leads the stronger pulse by 80 ps, illustrating time reversal and magnification

power of the time lens for controlling and shaping optical pulses.

Acknowledgments: This work was supported by the Air Force Office of Scientific Research, under contract number AF F49620-92-J-099.

15th December 1992

M. T. Kauffman, A. A. Godil, B. A. Auld, W. C. Banyai and D. M. Bloom (*Edward L. Ginzton Laboratory, Box 67, Stanford University, Stanford, CA 94305, USA*)

References

1 TREACY, E. B.: 'Optical pulse compression with diffraction gratings', *IEEE J. Quantum Electron.*, 1969, **QE-5**, pp. 454–458
2 KOLNER, B. H., and NAZARATHY, M.: 'Temporal imaging with a time-lens', *Opt. Lett.*, 1989, **14**, pp. 630–632
3 GODIL, A. A., AULD, B. A., and BLOOM, D. M.: IEEE Lasers and Electro-optics Society annual meeting, Boston, MA, 16th–19th November 1992
4 HERRIOTT, D., and SCHULTE, H. J.: 'Folded optical delay lines', *Appl. Opt.*, 1965, **4**, pp. 883–889
5 BRACEWELL, R. N.: 'The Fourier transform and its applications' (McGraw-Hill, New York, 1986), pp. 121–122
6 RODWELL, M. J. W., BLOOM, D. M., and WEINGARTEN, K. J.: 'Subpicosecond laser timing stabilization', *IEEE J. Quantum Electron.*, 1989, **QE-25**, pp. 817–827

LOW LOSS, HEAT-RESISTANT OPTICAL WAVEGUIDES USING NEW FLUORINATED POLYIMIDES

T. Matsuura, S. Ando, S. Sasaki and F. Yamamoto

Indexing terms: Optical waveguide, Polyimide, Optical loss, Refractive index control

Two types of polymer ridge optical waveguide are prepared using new fluorinated polyimides with excellent transparency and refractive index controllability. One has a polyimide core with a refractive index n of 1·573 and an SiO_2 undercladding layer. The other has a polyimide core (n = 1·521) and a polyimide undercladding layer (n = 1·520). These waveguides exhibit a low loss of 0·3 dB/cm at 1·3 μm. In addition, they have high thermal stability because of high temperature curing (above 350°C).

Introduction: Polymer waveguides have been investigated for use as flexible and low cost optical interconnects, and optoelectronic integrated circuits (OEICs) [1]. Booth [2] reported multimode waveguides with a loss of 0·25 dB/cm at 0·83 μm by using poly(methyl methacrylate) (PMMA), which had previously been used as a low loss optical fibre material [3]. Imamura *et al.* [4] fabricated a singlemode waveguide with a loss of less than 0·1 dB/cm at 1·3 μm by using deuterised and fluorinated PMMA. Recently, Sullivan [5] fabricated thermally-stable ridge waveguides with a loss of 0·3 dB/cm at 0·83 μm by using polyimide, which has been widely used as dielectrics in high-density interconnection modules. Reuter *et al.* [6] reported using polyimide as a waveguide material with a loss of 0·1 dB/cm at 0·63 μm by removing the solvent at 90°C. The loss increases around 3 dB/cm, however, after curing at 300°C.

We have synthesised new fluorinated polyimides for use as material for optical interconnects and OEICs. These polyimides exhibit excellent optical transparency in the visible region (0·7 dB/cm at 0·63 μm after curing at 350°C) and low water absorption (0·2%) due to polyimide fluorination.* Low

* MATSUURA, T., ANDO, S., SASAKI, S., and YAMAMOTO, F.: 'Polyimides derived from 2,2'-bis(trifluoromethyl)-4,4'-diaminobiphenyl. 4. Optical properties of fluorinated polyimide thin films', submitted to *Macromolecules*

water absorption in waveguide materials is very important for stabilising optical properties. This Letter describes the light absorption of fluorinated polyimides in the near-infrared region and also discusses the optical losses of the ridge waveguides at 1·3 μm.

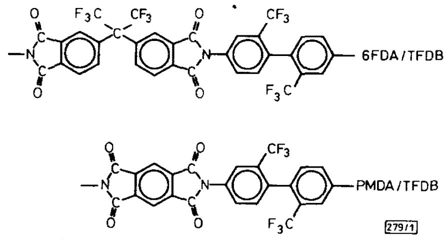

Fig. 1 *Fluorinated polyimides for waveguides*

Optical transparency: The newly developed polyimides are 6FDA/TFDB and PMDA/TFDB (Fig. 1), and their copolymers [7]. Fig. 2 shows the light absorption spectrum of 6FDA/TFDB cured at 200°C. A 10 wt% acetone-d_6 solution was used in measuring light absorption. Acetone-d_6 was used as the reference. Three peaks are observed in the near-infrared region: the third harmonics of the stretching vibration of the C–H bond ($3\nu_{CH}$, 1·1 μm), the combination of the second harmonics of the stretching vibration and the deformation vibration of the C–H bond ($2\nu_{CH} + \delta_{CH}$, 1·4 μm), and the second harmonics of the stretching vibration of the C–H bond ($2\nu_{CH}$, 1·65 μm). There are no clear peaks, however, at the telecommunication wavelengths of 1·3 and 1·55 μm. The loss at 1·3 μm of 6FDA/TFDB due to the harmonics of infra-red vibration absorption is estimated to be less than 0·1 dB/cm as calibrated with the known optical loss of 0·7 dB/cm at 0·63 μm [7].

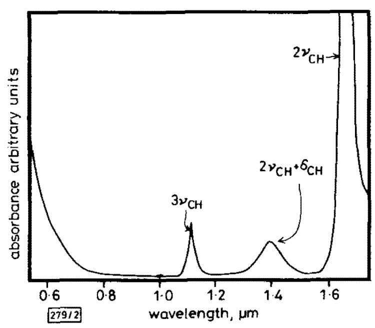

Fig. 2 *Light absorption spectrum of 6FDA/TFDB cured at 200°C*

Refractive index control: Fig. 3 shows the refractive indices of the polyimides and their copolymers at 1·3 μm. The refractive index n can be controlled precisely by changing 6FDA/TFDB content between 1·520 and 1·573.

Waveguide fabrication: Two types of ridge waveguide, guide I and guide II, were prepared. Guide I consists of PMDA/TFDB core ($n = 1{\cdot}573$, 15 μm wide, 10 μm thick, and cured at 350°C) with SiO_2 undercladding layer (3 μm thick). Guide II consists of a high refractive index copolyimide core (6FDA/TFDB : PMDA/TFDB = 9 : 1, $n = 1{\cdot}521$, 50 μm wide, 10 μm thick, and cured at 380°C), and a low refractive index 6FDA/TFDB undercladding layer ($n = 1{\cdot}520$, 4 μm thick, and cured at 380°C). The fabrication process is as follows. The polyimide or copolyimide precursor, an N,N-dimethylacetamide solution of poly(amic acid), is spin-cast on a silicon substrate with an oxidised surface layer or with a polyimide surface layer, and then heated for curing. High thermal stability in these waveguides is achieved by high temperature curing (above 350°C). Ridge waveguides are fabricated using conventional photolithography and dry etching techniques. Fig. 4 shows a scanning electron micrograph of guide I.

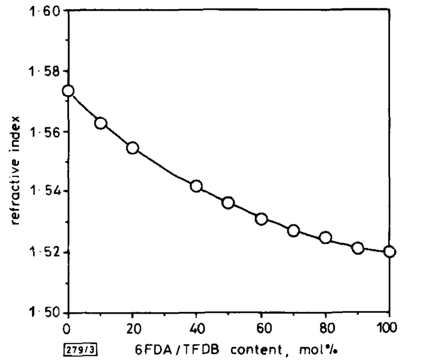

Fig. 3 *Refractive index of 6FDA/TFDB, PMDA/TFDB and their copolymers at 1·3 μm*

Optical loss: Local measurements were performed using a laser diode as a 1·32 μm light source. The light was introduced into the waveguide using singlemode fibres with a mode-field diameter of 8 μm. The input fibre was then precisely butted against the waveguide. The propagation losses were measured using the cut-back method and calculated from the slopes in Fig. 5 (transmission losses against waveguide length). Guides I and II have losses at 1·3 μm of 0·34 and 0·32 dB/cm, respectively.

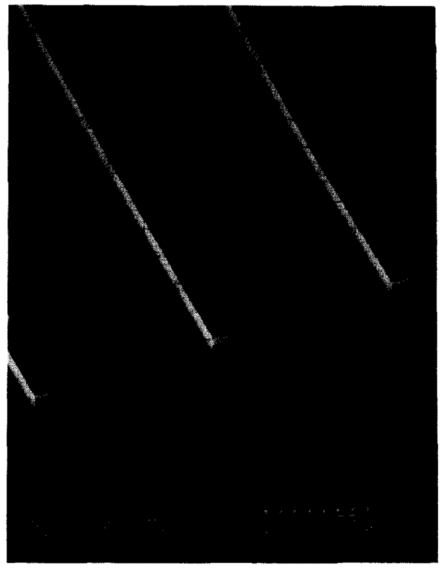

279/4

Fig. 4 *Scanning electron micrograph of a guide I ridge waveguide with a PMDA/TFDB core and SiO_2 undercladding layer*

Conclusion: Heat-resistant ridge waveguides were fabricated using new fluorinated polyimides with excellent transparency and refractive index controllability. These high heat-resistant polyimide waveguides have optical losses of around 0·3 dB/cm at 1·3 μm. Low loss, singlemode embedded waveguides with high thermal stability can be fabricated using these copolymides.

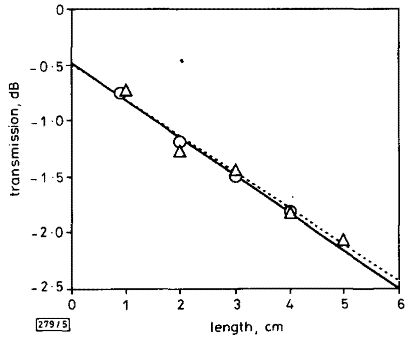

Fig. 5 *Transmission losses of ridge waveguides at 1·3 μm*
—○— guide I
--△-- guide II

Acknowledgment: We wish to thank T. Izawa and Y. Ishii for their helpful comments. We also wish to thank H. Takahara and F. Shimokawa for their useful comments and discussions. Thanks also to H. Hirata for help with the loss measurement, and S. Imamura and M. Hikita for help with the waveguide fabrication.

8th December 1992

T. Matsuura, S. ando, S. Sasaki and F. Yamamoto (*NTT Interdisciplinary Research Laboratories, Musashino-shi, Tokyo 180, Japan*)

References

1 IZAWA, T.: 'Plastic planar waveguides for optical interconnects'. ECOC-IOOC 91, 1991, Web6-1
2 BOOTH, B. L.: 'Low loss channel waveguides in polymers', *J. Lightwave Technol.*, 1989, **LT-7**, (10), pp. 1445–1453
3 KAINO, T.: 'Preparation of plastic optical fibers for near-IR region transmission', *J. Polym. Sci.*, Part A, 1987, **25**, pp. 37–46
4 IMAMURA, S., YOSHIMURA, R., and IZAWA, T.: 'Polymer channel waveguides with low loss at 1·3 μm', *Electron. Lett.*, 1991, **27**, pp. 1342–1343
5 SULLIVAN, C. T.: 'Optical waveguide circuits for printed wire-board interconnections', *SPIE*, 1988, **994**, pp. 92–100
6 REUTER, R., FRANKE, H., and FEGER, C.: 'Evaluating polyimides as lightguide materials', *Appl. Opt.*, 1988, **27**, (21), pp. 4565–4571
7 MATSUURA, T., YAMADA, N., NISHI, S., and HASUDA, Y.: 'Polyimides derived from 2,2'-bis(trifluoromethyl)-4,4'-diaminobiphenyl. 3. Property control for polymer blend and copolymerization of fluorinated polyimides', to be published in *Macromolecules*

HIGH EFFICIENCY HIGH-SPEED PHOTODETECTION IN A MONOLITHICALLY INTEGRATABLE InGaAs/InP MQW LASER STRUCTURE AT 1·5 μm

K. A. McGreer, S. Charbonneau, M. Davies, G. Aers, B. Takasaki, D. Landheer, D. Moss, M. Dion and A. Delage

Indexing terms: Integrated optoelectronics, Photodetectors, Semiconductor lasers

Time-resolved photocurrent measurements in a reverse biased InGaAs/InP ridge waveguide multiquantum well *pin* laser structure at 1·54 μm are reported. The pulse response of this monolithically integratable detector is ~150 ps FWHM with an internal quantum efficiency of ~100% at reverse bias voltages of ~5 V.

The effective incorporation of detectors, lasers, modulators and optical amplifiers is the central challenge of the monolithic integration of photonic circuits. Photodetectors made from reverse biased laser structures have potential application in these circuits. Such photodetectors may permit considerable reduction of growth and fabrication complexity as the same layer structure may perform different functions. These detectors depend on the quantum confined Stark effect (QCSE). In multiquantum well (MQW) semiconductor devices this effect has provided the physical basis for several new electro-optic devices including tunable detectors [1–4], electroabsorption modulators [5] and self-electro-optic effect devices (SEED) [6–7]. Key requirements are efficiency and speed. The ultimate speed at which photodetectors can operate is determined by the rate at which photogenerated carriers can be ejected from the quantum well and swept out of the active region. It is therefore important to measure the response time of these structures in order to optimise their design. We report the photoconductive response of a planarised ridge waveguide InGaAs/InP MQW laser at 1·54 μm and demonstrate that such a device can make a highly efficient and fast photodetector when operated under reverse bias.

The layer structure was grown by low pressure MOVPE by Epitaxial Products International (UK) and is shown schematically in Fig. 1, under flat band conditions. Broad area laser data are shown in Fig. 2. The threshold current density at 1000 μm cavity length is ~700 A/cm^2 with internal losses of 14 cm^{-1}. Nonplanarised ridge waveguide lasers fabricated from this material typically had threshold currents of 35 mA for a 3 × 300 μm^2 cavity with uncoated facets. To investigate the dynamics of photogenerated carriers, time resolved photoconductivity (PC) measurements were performed on a planarised ridge waveguide structure shown schematically in Fig. 3. These devices were fabricated by a selfaligned wet etch process and planarised with polyimide. The device geometry was designed to minimise parasitics and has been reported previously [1]. The device (3 μm wide by 250 μm long) when operated under forward bias had a laser threshold current of 22 mA and a leakage current of 4 μA at −5 V.

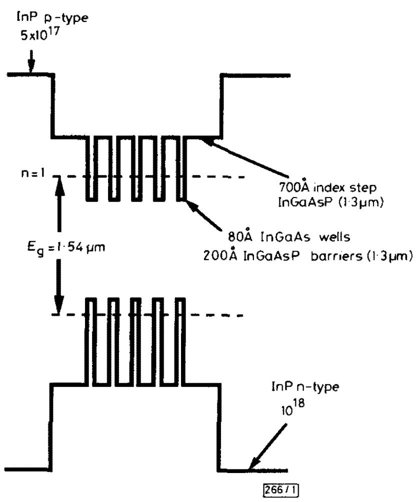

Fig. 1 *Schematic band diagram of MQW laser structure*

To measure the pulse response of the detector, the output (pulse width <15 ps, λ = 1·52 μm, repetition rate = 76 MHz) of a mode locked, synchronously pumped colour centre laser was coupled into a polarisation preserving singlemode fibre which was then butt coupled to the wave guide of the device. The optical pulse energy was ~10 meV above the EL1-HH1 energy transition. The device was mounted on a microwave